SNRM
Sistema Nacional de Resonancia Magnética

Ministerio de Ciencia, Tecnología e Innovación Productiva
Secretaría de Articulación Científico Tecnológica

IFEG CONICET UNC

UNC FAMAF

Principios Básicos de RMN en sólidos destinado a usuarios

Gustavo Monti

Fa.M.A.F. – Universidad Nacional de Córdoba – Argentina

APPLICATIONS

We will show examples of application in the following organic compounds and drugs of pharmaceutical interest.

Chlorpropamide, is indicated as adjunctive therapy to diet to controlhyperglycemia in diabetes mellitus patients with insulin-dependent diabetesformerly stable adult who can not be controlled satisfactorily by diet alone.

Cortisone acetate, is an antiinflammatory agent used in the treatment of allergy and collagen diseases.

Sildenafil citrate, commercially known as Viagra, used to treat erectiledysfunction, is an inhibitor of phosphodiesterase type 5.

4'-methyl-2'-nitroacetanilide

Formoterol fumarate: Formoterol acts on receptors in the lungs called beta 2receptors. When formoterol stimulates the receptors causes the muscles relax the airways allowing them to open. Easier to breathe in conditions of asthma,emphysema and chronic bronchitis.

Prednisolone: Prednisolone is a synthetic corticoesteroride.

The corticoesteroids are natural substances produced by the adrenal glands. Corticosteroids have potent anti-inflammatory properties and are used in a wide variety of inflammatory conditions such as arthritis, asthma, bronchitis, colitis, certain types of reactions in the skin, and allergic or inflammatory conditions of the eyes and nose.

2-amino benzoic acid, is used in the formulation of certain pharmaceuticals.

[S, S]-ethambutol dihydrochloride: a drug active against Mycobacteriumtuberculosis. Not well understood how it works.

Azithromycin: a next-generation macrolide (azaleas) that acts by inhibiting protein synthesis and translocation of bacterial peptide. Effective respiratory tract infections upper and lower (including otitis media, sinusitis, pharyngitis, bronchitisand pneumonia), skin and soft tissue sexually transmitted diseases and generallyuncomplicated in bacterial infectious processes caused by susceptible bacteria, aerobic, anaerobic, gram-positive, gram-negative, non-multiresistant chlamydiaand Neisseria.

Polimorphs

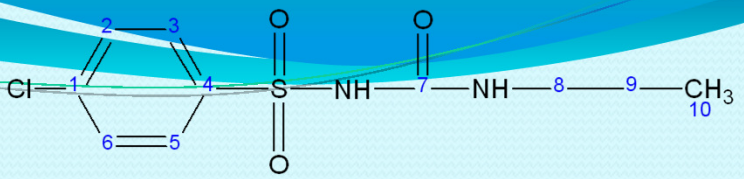

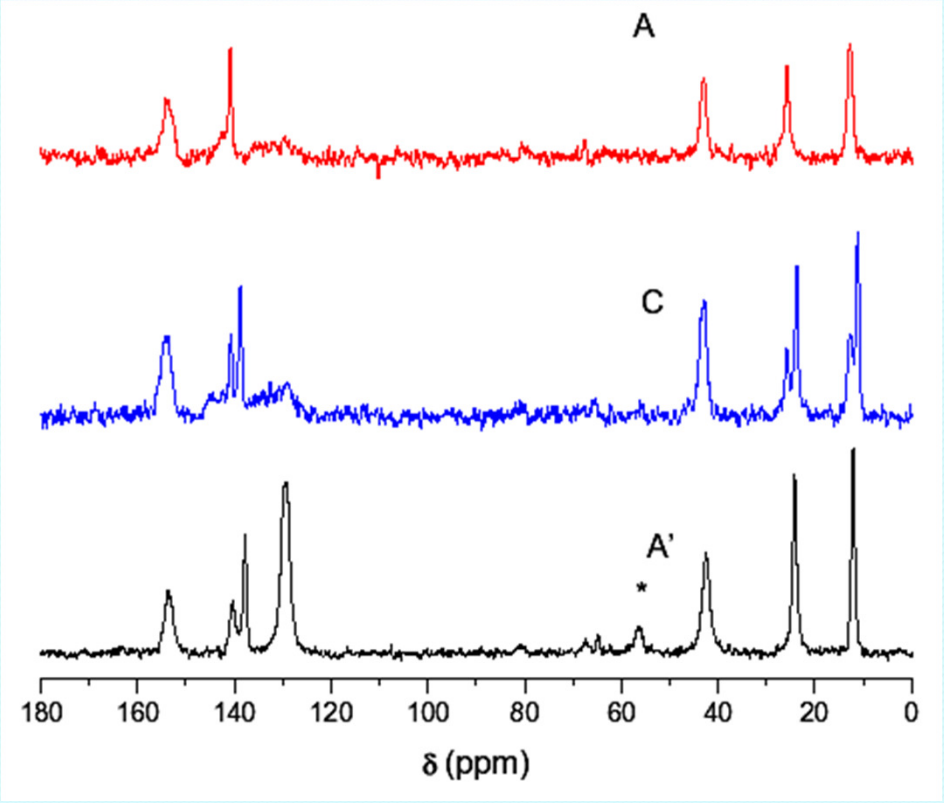

CPMAS spectra of 13C in various forms of chlorpropamide. Polymorph C has more than one molecule in the asymmetric unit cell. Polymorph A 'would have a single molecule in the asymmetric unit cell as A, but unlike the latter resonance ca130 ppm indicate a high mobility of the phenyl group . Rotational bands are indicated by asterisks.

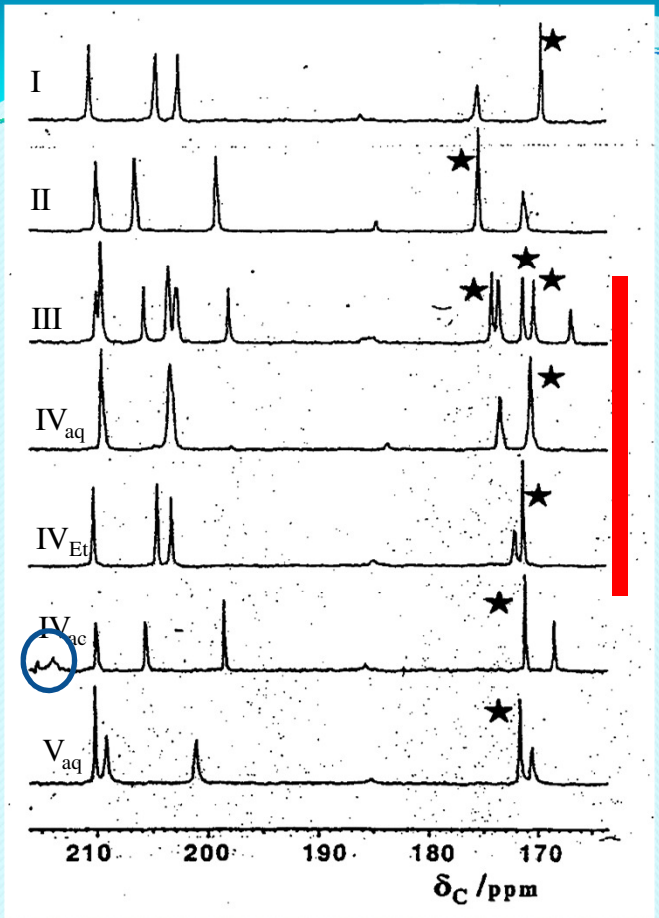

Detail of the high frequency region of the CPMAS spectra of 13C in various forms of cortisone acetate. The stars indicate the lines of the C-22.

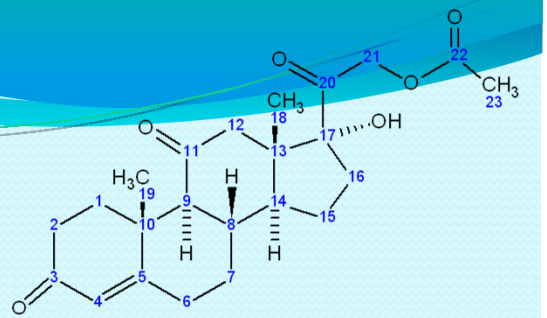

The additional information given by these spectra, unlike X-ray and vibrational spectroscopy are:

For Form III, whose structure is not determined by X-ray diffraction, we can see that there are three molecules per asymmetric unit cell, while in all other forms only one of such molecules.

Solvate peaks are clearly present in the acetone solvate (as IVAC the peak run to the left is the carbonyl carbon of acetone solvate)

The intensities of the peaks on the right side of the spectra appear to intercalate at random, this effect is related to the nature of intermolecular hydrogen bonds.

This latter point gives the following conclusion: IVaq forms, IVEt and two of the three asymmetric molecules in form III form hydrogen bonds through the carbonyl group at C-3, this says that there are connections "head-to-tail", while the third asymmetric molecule of form III form hydrogen bonds with connection" head-to-head ", ie through the carboxyl group at C-22 (RK Harris et al. 1992).

Interaction with water vapor

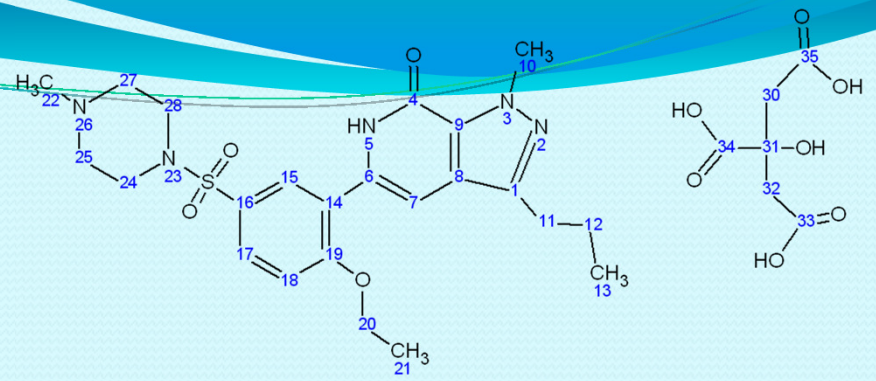

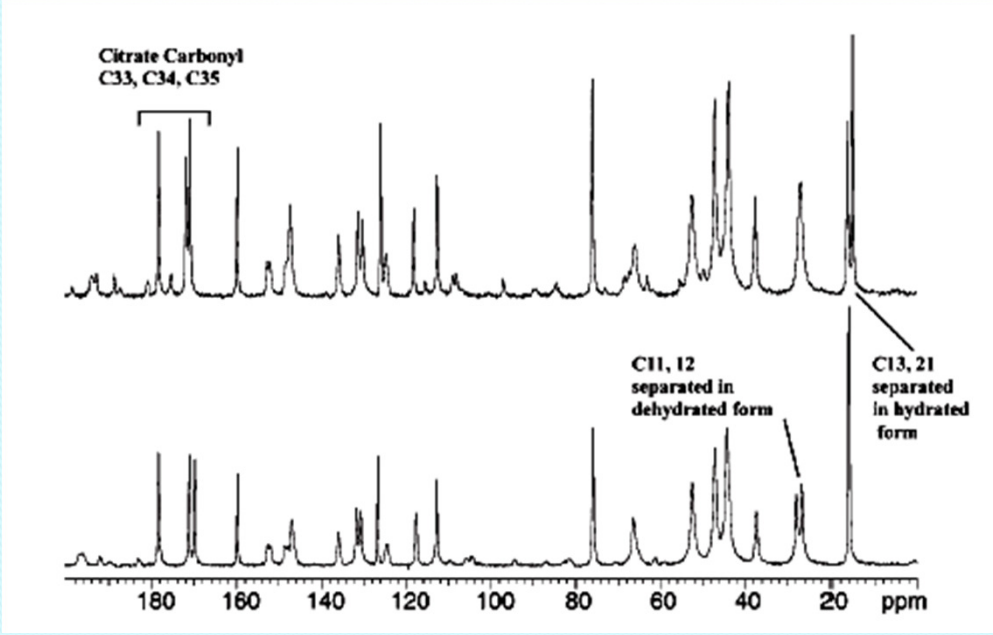

13C CPMAS spectra of sildenafil citrate. Top: sample stored at 88% relative humidity for 7 days. Bottom: sample stored at 0% relative humidity for 7 days. It highlights the carbons most affected by the change in water content (see diagram of the molecule) (DC Apperley et al. 2005).

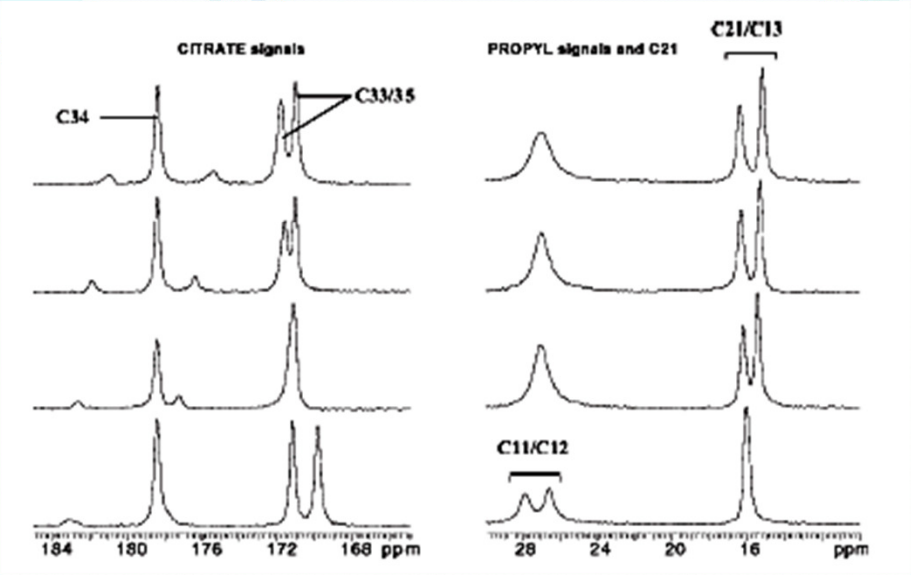

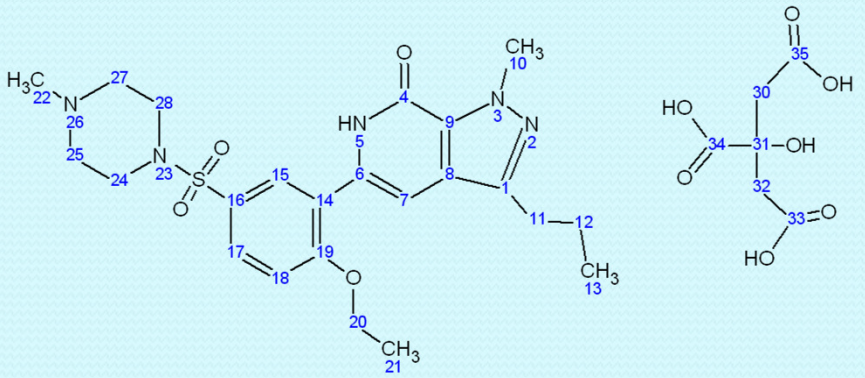

Details of the 13C CPMAS spectra of sildenafil citrate. Left: region of the carboxyl groups of citrate. Right: region of the propyl group (C21 is also included) of the molecule of sildenafil. From top to bottom the conditions of the samples were: kept at 88%RH for 7 days, kept at 88% RH for 3.5 days, as it was originally collected, stored at 0% RH for 7 days. Changes in chemical shifts of C33/35 is indicative of the formation of hydrogen bonds. The changes in the region of the propyl group are indicative of changes in the environment of these groups, probably slight changes in average conformation of the group due to the presence of water molecules (DCApperley et al. 2005).

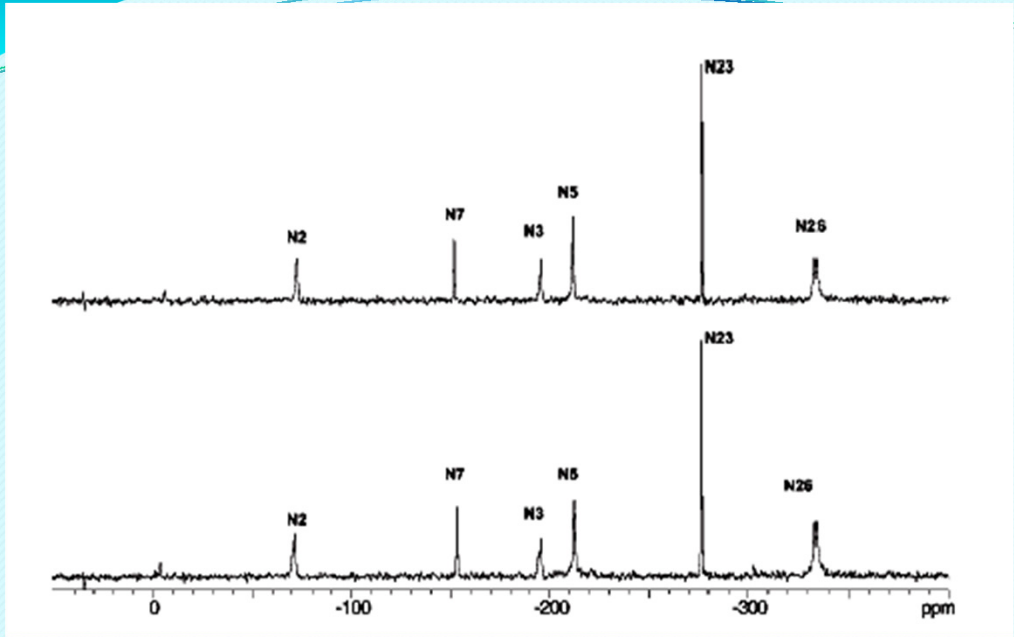

15N CPMAS spectra of the samples sildenafil citrate after stored at 88% RH (top) and 0% RH (bottom) for 7 days. 15N2 and 15N3 nitrogens are clearly identifiable in the sample stored at 0% RH, as have the characteristic doublet due to coupling 1:2 residual dipolar 14N-15N. The similarity of the 15N chemical shifts in all sildenafil nitrogen at 0% and 88% RH is consistent with only small changes in estrucutra crystalline in the solid state at different levels of hydration (DC Apperley et al. 2005).

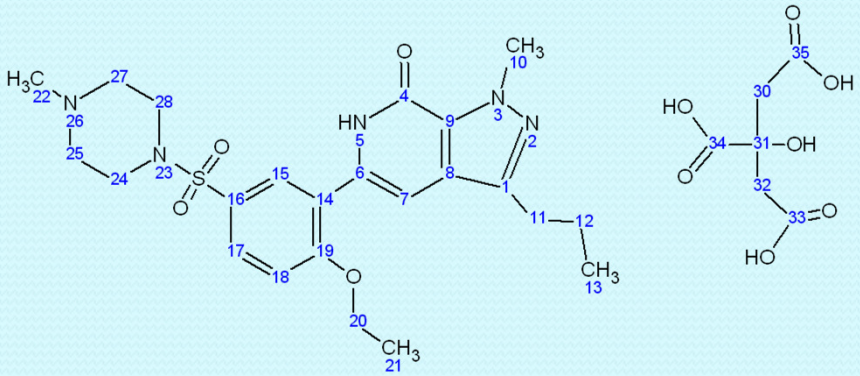

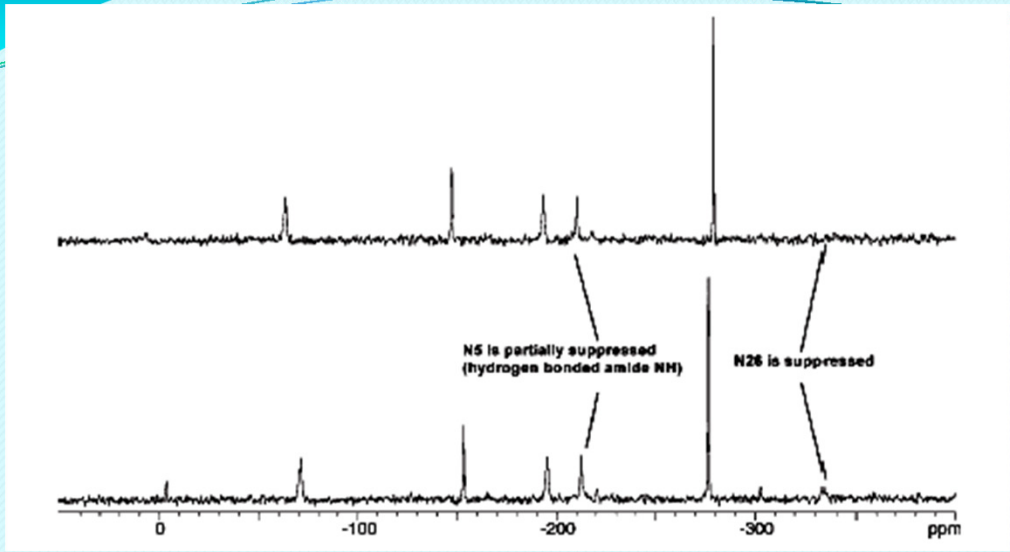

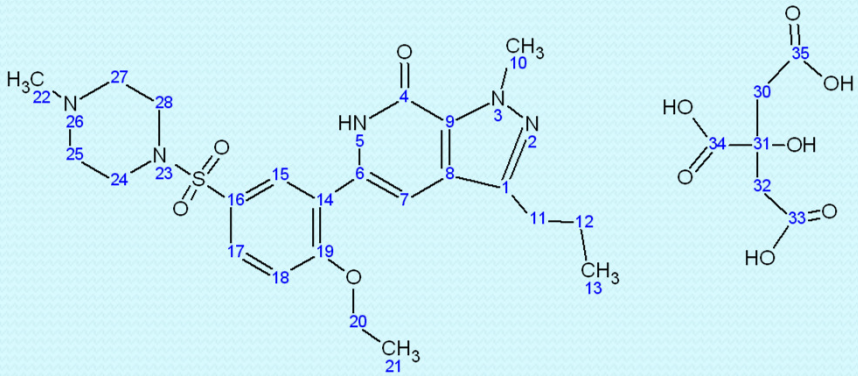

Dipolar spectra obtained with 15N desfazaje samples sildenafil citrate after 88% conserved HR (top) and 0% RH (bottom) for 7 days. In such experiments the protonated nitrogen signals are reduced in intensity or are not detected directly. The partial reduction of the N5 signal (-212 ppm) is consistent with the existence of hydrogen bonds between hydrogen 5-NH and the adjacent oxygen of the phenyl ring, resulting in a lengthening of the NH bond, making this last less efficient dipolar coupling NH. The N2 signal (-72 ppm) is not affected by the experiment. The signal from the N26 (-333.5 ppm) is completely suppressed. These data indicate that protonation occurs only in the piperazine ring N26 (DC Apperley et al. 2005).

Localizing hidrogen atoms in hidrogen bonds

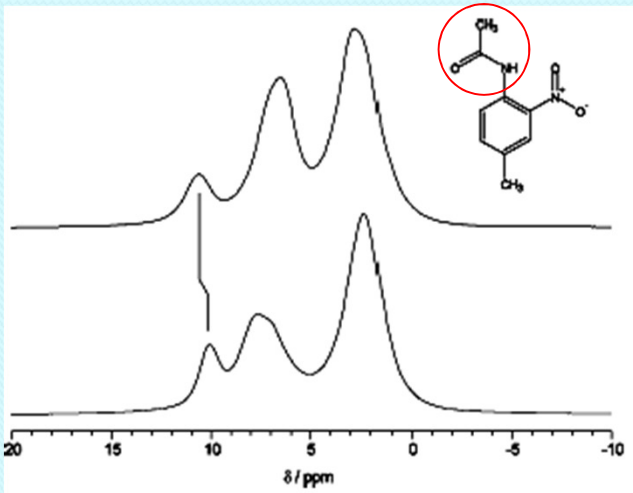

High-speed MAS spectrum of protons methylnitroacetanilide (MNA). Above, the white form. Below, the yellow form. The signal of hydrogen bond is to the left, with a chemical shift of 10.8 ppm (RK Harris et al. 2003).

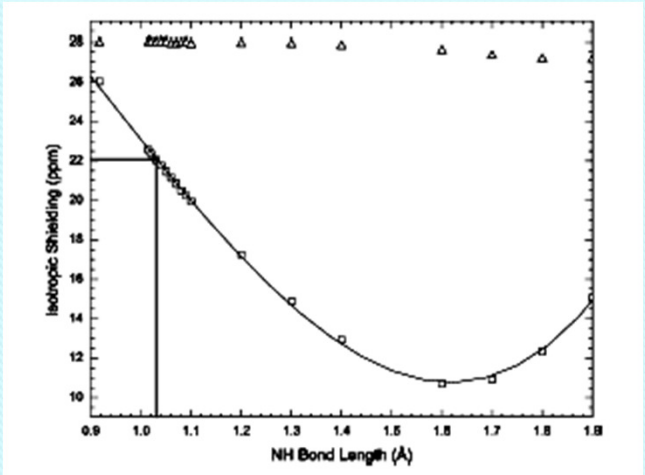

DFT Calculation of the isotropic shielding constant (in absolute scale) of the proton forming hydrogen bonds in the white form of MNA, plotted as a function of distance for the dimer NH. The horizontal line is the experimental value of the corresponding chemical shift (RK Harris et al. 2003).

Quantification

As an example we take the formoterol fumarate, which exists in a stable dihydrate (FFD) and a hygroscopic anhydrous form (FFA). These can be distinguished by the signs of the carboxyl carbons of fumarate (DC Apperley et al. 2004).

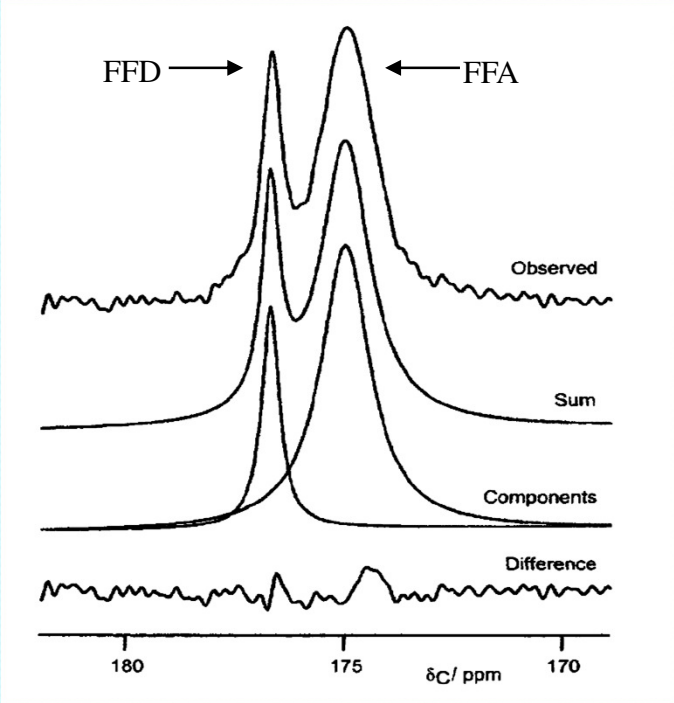

Detail of the region of 175 ppm of 13C CPMAS spectrum of a mixture of FFA and FFD (DC Apperley et al. 2004).

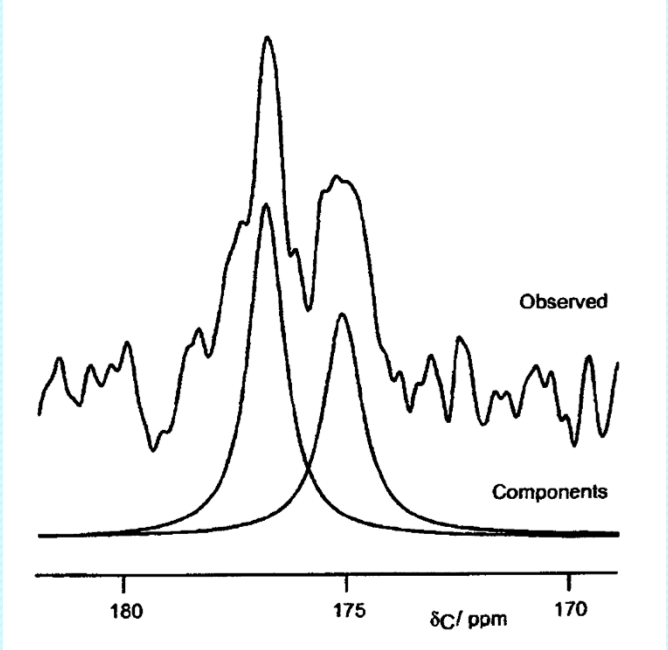

13C CPMAS spectrum (high frequency region only) of a mixture FFA / FFD total composition in a mass of 2% lactose. The deconvolution indicates that the sample has a 57 ± 4% of FFD (DC Apperley et al. 2004).

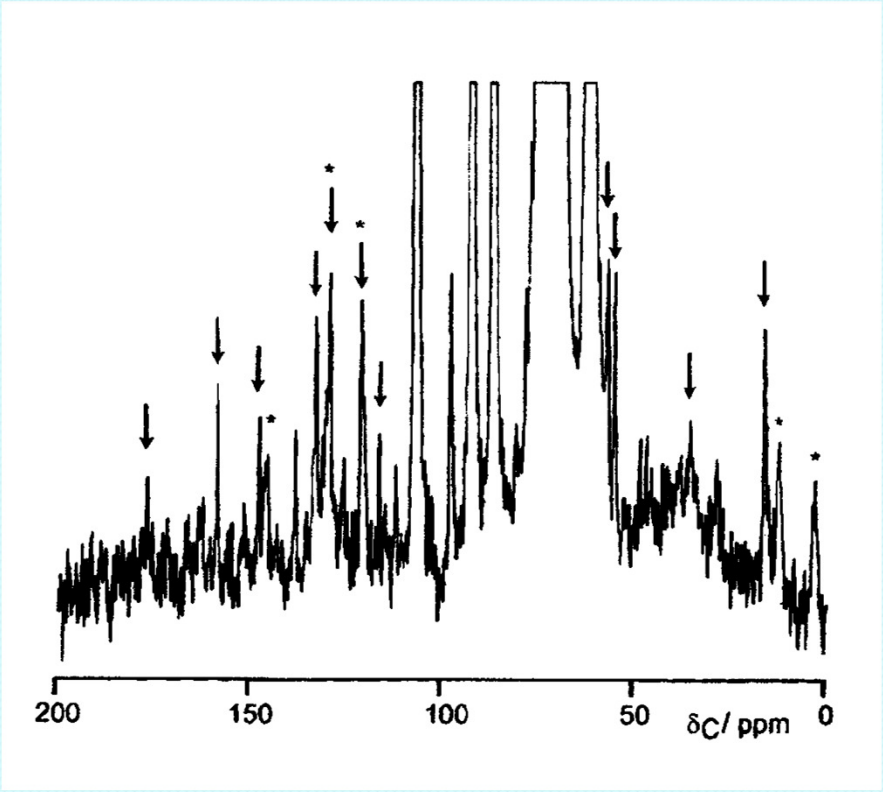

13C CPMAS spectrum of FFD 0.45% lactose. Rotational bands are indicated by asterisks and the signal with vertical arrows FFD (DC Apperley et al. 2004).

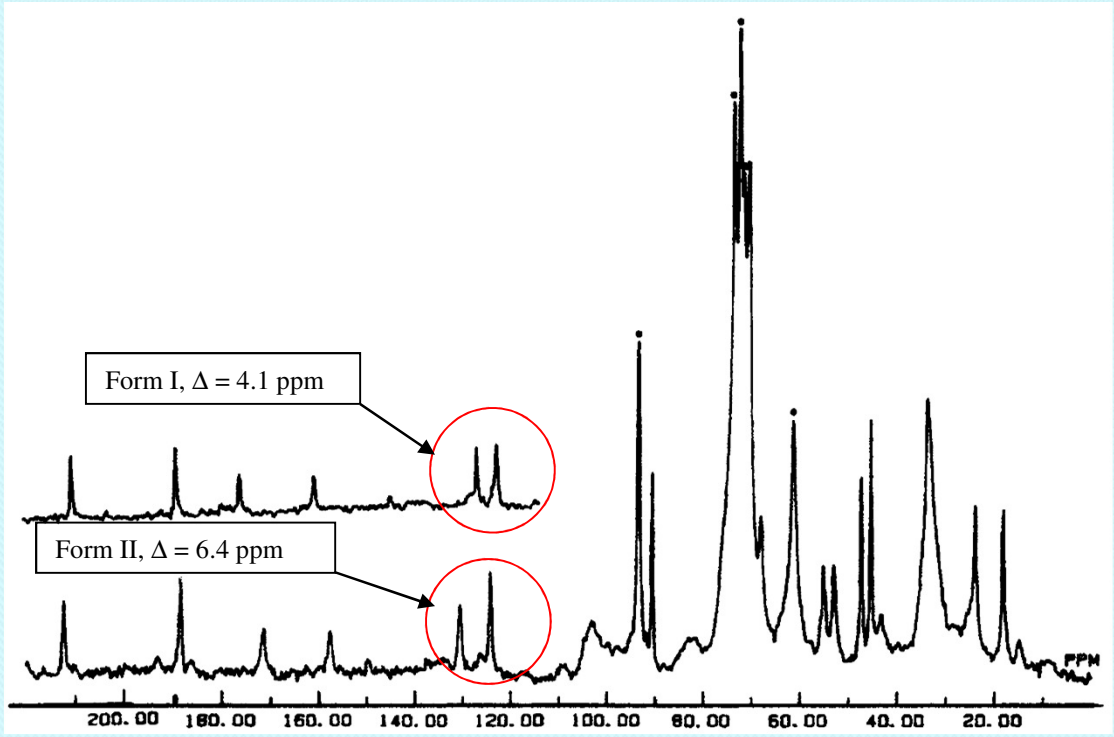

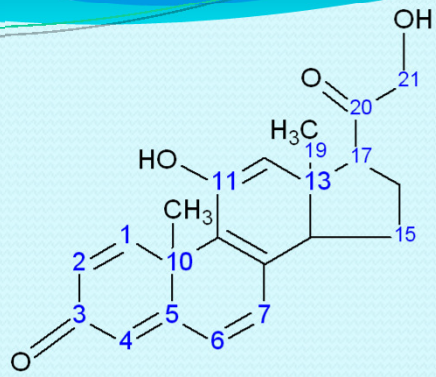

Espectro CPMAS de 13C de tabletas de prednisolone provenientes de dos compañias farmaceúticas. El inserto muestra la region de mayor diferencia entre la forma I y la forma II de prednisolone y muestra que este producto contiene prednisolone en la forma I. Los asteriscos indican las resonancias del excipiente (P. J. Saindon et al. 1993). A case of quality control failure?

Tautomerism

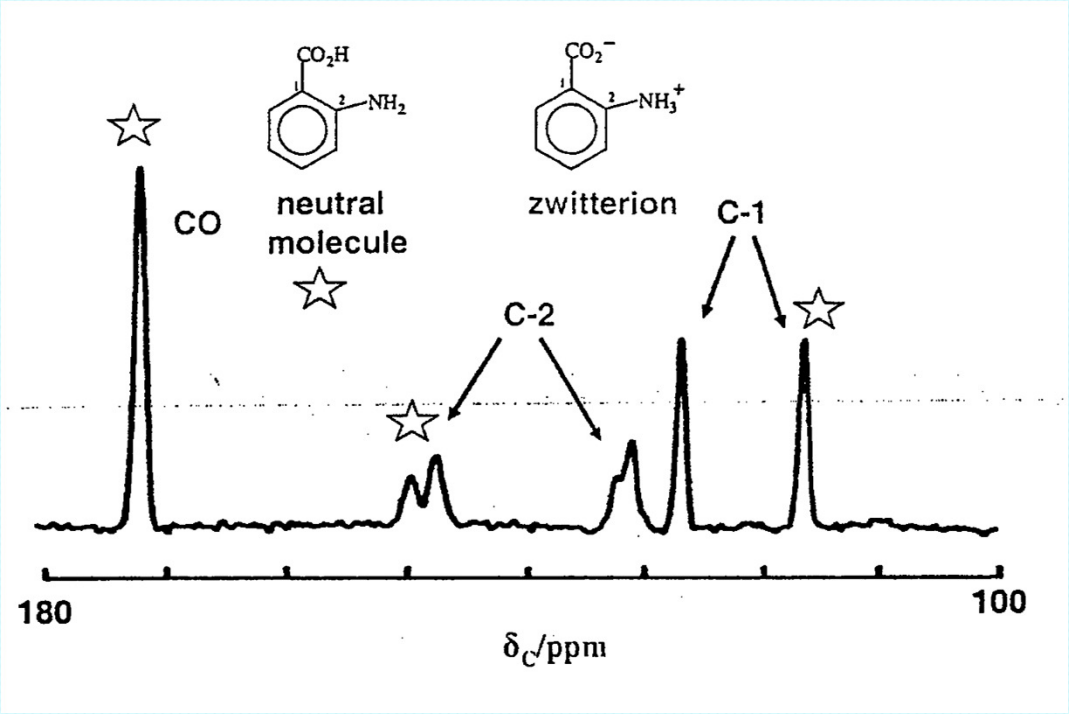

13C CPMAS spectrum of form I 2-aminobenzoic acid. The resonances of the neutral molecules are indicated by stars (RK Harris et al. 1987)

Transitions between polimorphs

NMR experiments as a function of temperature can be used to keep track of a transformation between polymorphs. An example for this is the [S, S]-ethambutoll dihydrochloride (EMB) (JM-perming Rubin et al. 2004). This compound has four polymorphs, two of them suffer from a reversible phase transformation, fast, enantiotropic.

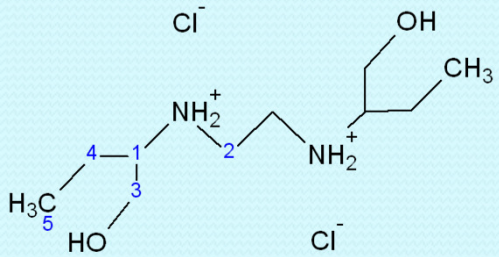

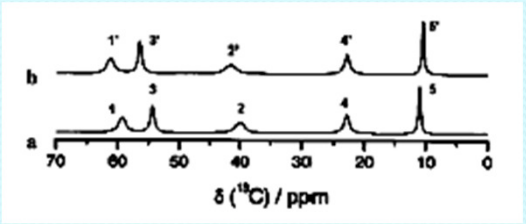

13C CPMAS spectrum of form II (a) at 50 ℃ (indicated by X) and the I to 80 ºC (atoms indicated by X‘, where X is the numbering of atoms according to the molecular scheme shown (JM Rubin -perming et al. 2004).

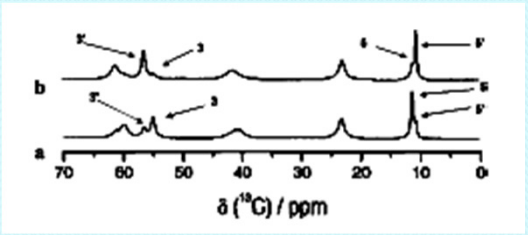

13C CPMAS spectra at about 74 C with a temperature gradient purposely placed to show the transformation between form II (a) (indicated by X) and form I (b) (atom indicated by X‘, where X is the numbering of atoms according to the molecular pattern shown) where the average temperature for (b) is slightly higher than for (a) (JM Rubin-perming et al. 2004).

Amorphous compounds: NMR vs X Ray

NMR is a good alternative to X-rays especially in case of amorphous systems. Azithromycin, for example, exists in three forms, two crystalline (monohydrate and dihydrate) and amorphous (anhydrous).

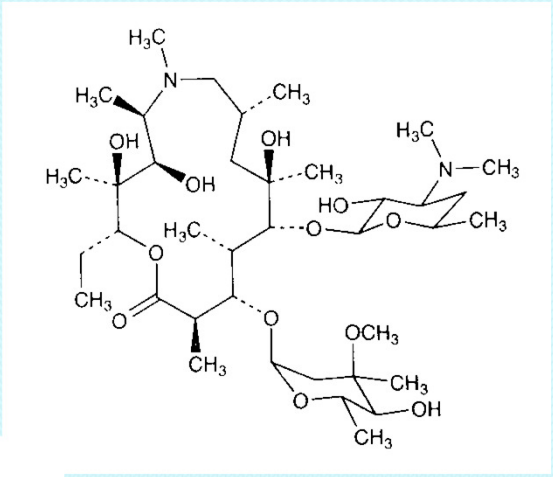

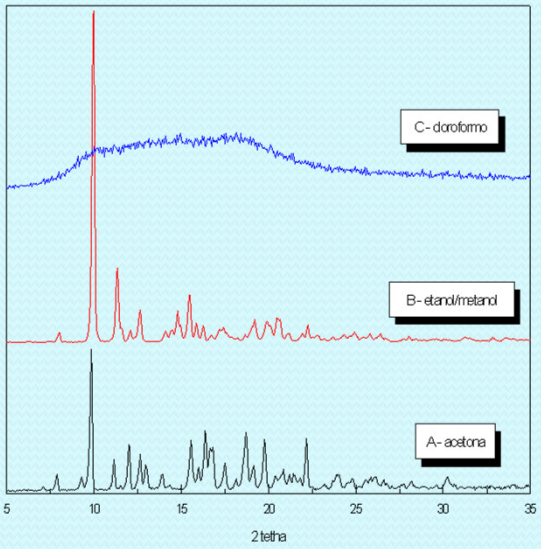

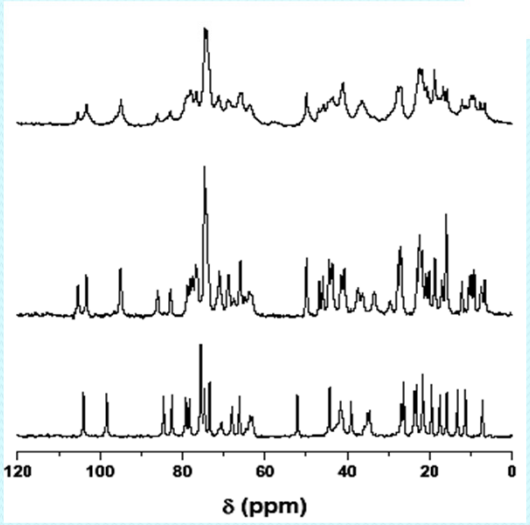

spectra of three forms of azithromycin ((a) dihydrate, (b) monohydrate, (c) amorphous). X-rays right, left (region 0-120 ppm) 13 C CPMAS NMR (Cuffini SL et al. 2002).

Enalapril:β-Cyclodextrin Complex

Ariana Zoppi, Claudia Garnero, Yamila Garro Linck, Ana K. Chattah, Gustavo A. Monti and Marcela R. Longhi. Carbohydrate Polymers. **86**, 716– 721 (2011). ISSN 0144-8617.

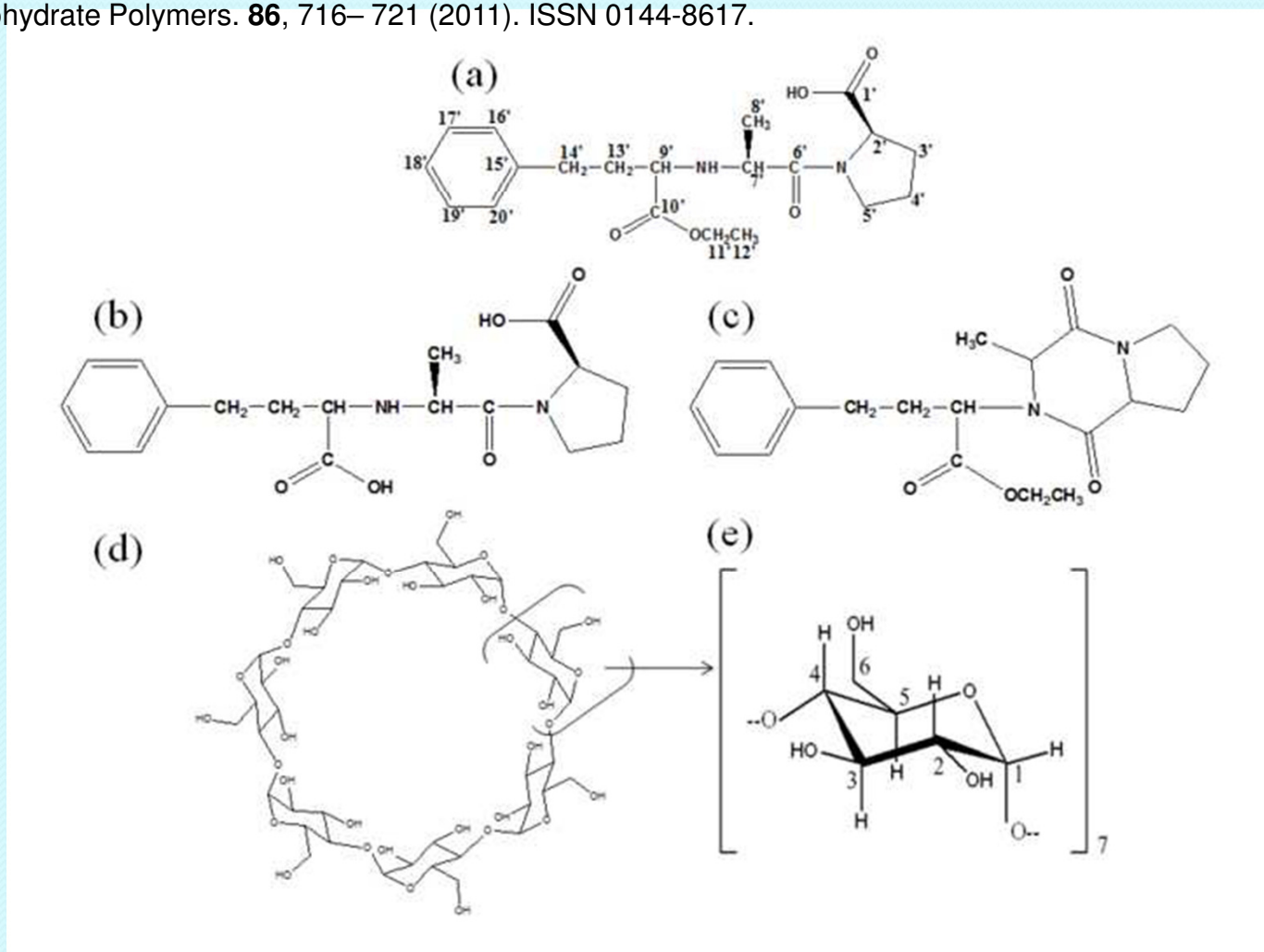

Molecular structure. (a) enalapril and carbon atoms numbering scheme, (b) enalaprilat and (c) enalapril diketopiperazine, (d) molecular structure of β-CD and (e) carbon atoms numbering scheme of β-CD.

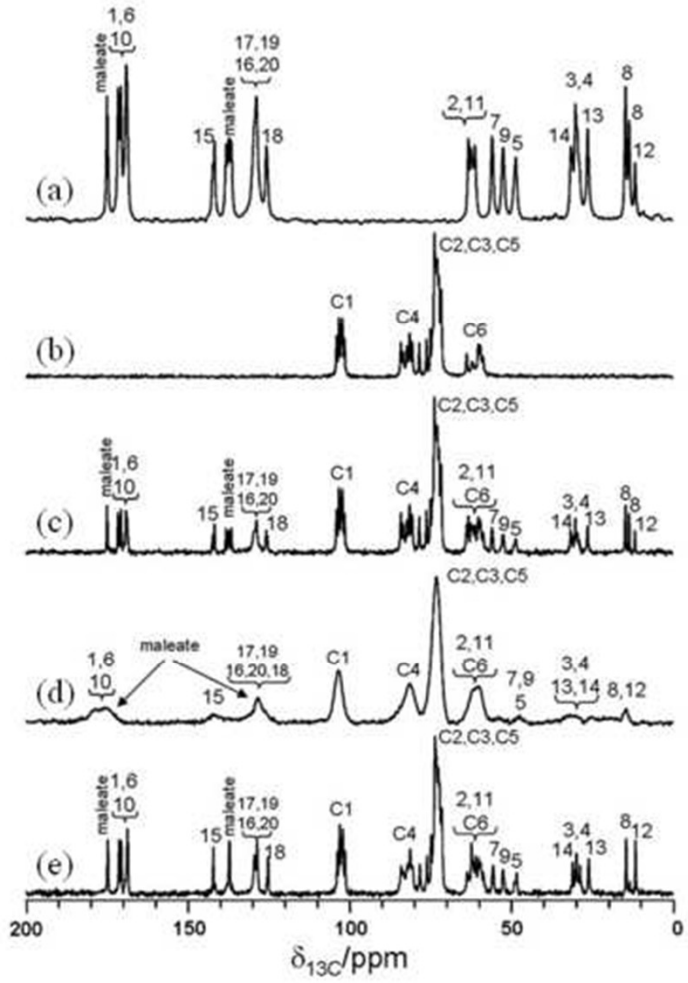

Solid state 13C CP MAS NMR spectra of (a) pure enalapril maleate, (b) pure β-CD, (c) enalapril maleate:β-CD physical mixture, (d) enalapril maleate:β-CD inclusion complex, (e) enalapril maleate:β-CD physical mixture after lyophilization of the pure components.

β-CD exhibits a complex spectrum (Fig. b) This fact may be correlated with distinct values of dihedral angles of the glycosidic α(1→4) bond for carbons 1 and 4, and with torsion angles describing the orientation of the hydroxyl groups

Fig. c shows that the characteristic resonances of enalapril maleate and β-CD are clearly distinguishable in the spectrum of the physical mixture. In the spectrum of the complex (Fig..d), the broadening of the peaks indicates that the complex is a new solid and amorphous form. The resonante changes could also be due to the complexation that induced the ring of β-CD to adopt a less distorted conformation with each glucose unit in a similar environment. The shift to higher frequencies observed for C(1), C(6) and C(10) atoms of enalapril maleate demonstrates a deshielding effect, which may be explained by the presence of hydrogen bond interactions between the carbonyl groups of enalapril maleate and the hydroxyl groups of β-CD.

Fig e): the lyophilization process did not introduce changes in the molecular environment of either the drug or the macromolecule.

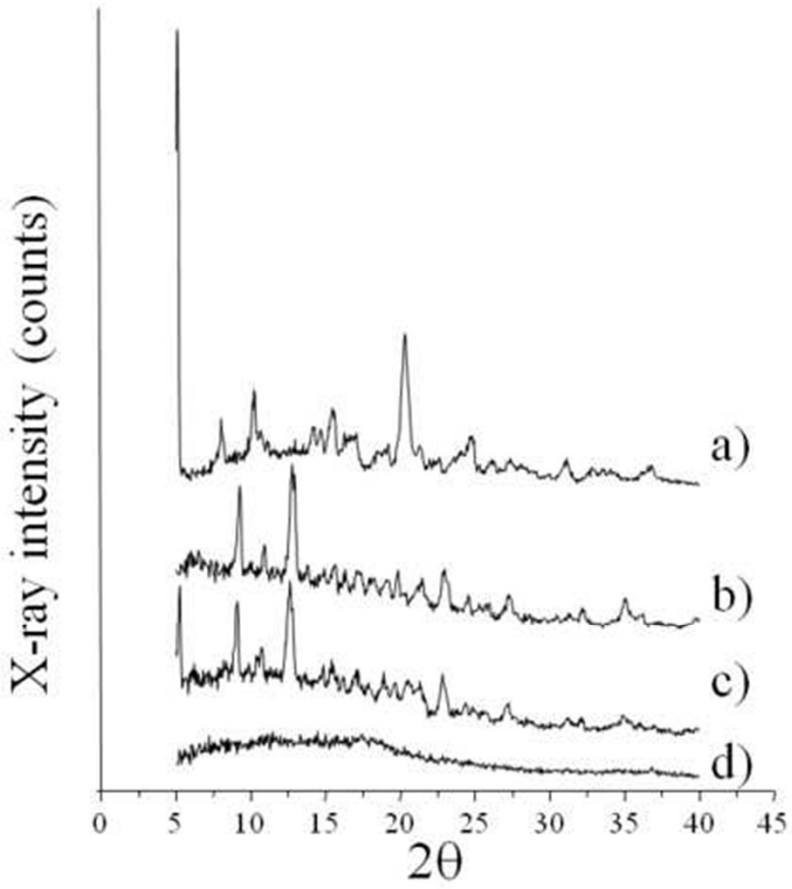

X-ray diffractograms (a) pure enalapril maleate, (b) pure β-CD, (c) enalapril maleate:β-CD physical mixture, d) enalapril maleate:β-CD inclusion complex.

Nitazoxanide

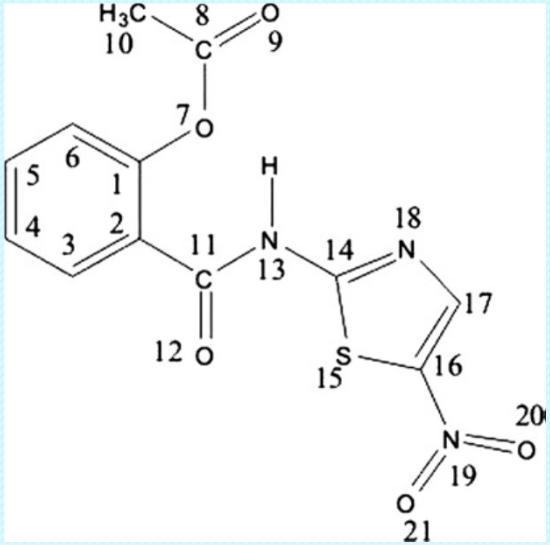

C atoms	CPMAS	CDCl3 (0.062 M)	Difference (SS-CDCl3)	DMSO-d_6 (0.065 M)	Difference (SS-DMSO-d_6)
1	148.3	148.7	-0.4	149.1	-0.8
2	122.5	123.6	-1.1	125.9	-3.4
3	133.9	130.7	3.2	30.3	3.6
4	127.0	126.8	0.2	126.4	0.6
4a	127.7	–	–	–	1.3
5	135.2	134.5	0.7	134.0	1.2
6	125.2	123.9	1.3	123.9	1.3
8	168.9	168.1	0.8	169.4	-0.5
10	22.2	21.2	1.0	21.2	1.0
11	163.0	162.9	0.1	165.8	-2.8
14	160.4	160.9	-0.5	162.3	-1.9
16	145.0	140.6	4.4	143.0	2.0
17	141.5	140.6	0.9	142.6	-1.1

Comparison of the 13C NMR chemical shifts (in ppm) of NTZ in solid and solution (CDCl3 and DMSO-d6) states.

The chemical shifts of seven of the 12 carbons of the molecule, C-1, C-4, C-5, C-6, C-8, C-10 and C-17, measured in the solid state are close to the values observed in both solutions indicating that the chemical environment around these carbons is very similar in the solid state and in solution . In particular, the C-8 carbonyl chemical shifts are similar, and this could indicate that the weak strength of the intermolecular bond between this carbonyl and the H-5', demonstrated in the crystal structure, does not affect the C-8 chemical shift value in the solid state.

Flavia P. Bruno, Mino R. Caira, Gustavo A. Monti, Diego E. Kassuha, Norma R. Sperandeo
Journal of Molecular Structure 984 (2010) 51–57

The C-2, C-11 and C-14 carbon chemical shifts measured in the solid state are close to the values observed in CDCl3 solution, but slightly different from the values observed in DMSO-d6 (Dsolid-solution: 3.4, 2.8 and 1.9 ppm, respectively). The observed DMSO-d6-induced shifts can be attributed to the usual solvents effects and to the formation of intermolecular interactions of the molecule of NTZ with DMSO-d6 through the amide proton.

C-3 showed similar chemical shifts in CDCl3 and DMSO-d6 solutions; but it is shifted to a high frequency in the solid state (Dsolid-solution: 3.2 and 3.6 ppm), and this could indicate a small change in the orientation of the amide group in the solid state

Very similar chemical shifts are observed for C-16 and C-17 in the 13C SNMR spectra, i.e. the signals merged in CDCl3, indicating a chemical equivalence of these carbons; however, two separate signals at 144.5 and 141.1 ppm with accompanying high frequency shifts of about 4 and 2 ppm, respectively, are observed for these carbons in the solid state, indicating that the chemical environments are different for these carbon atoms possibly due to further rigidities of the nitro group and thiazole ring in the solid state.

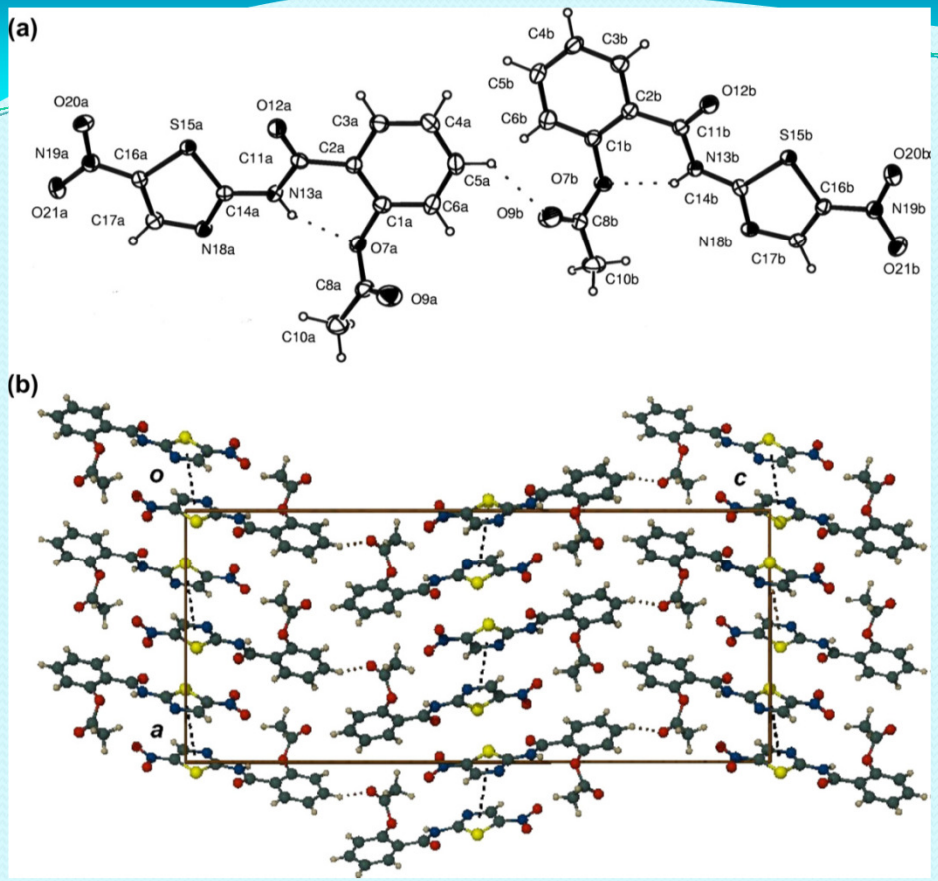

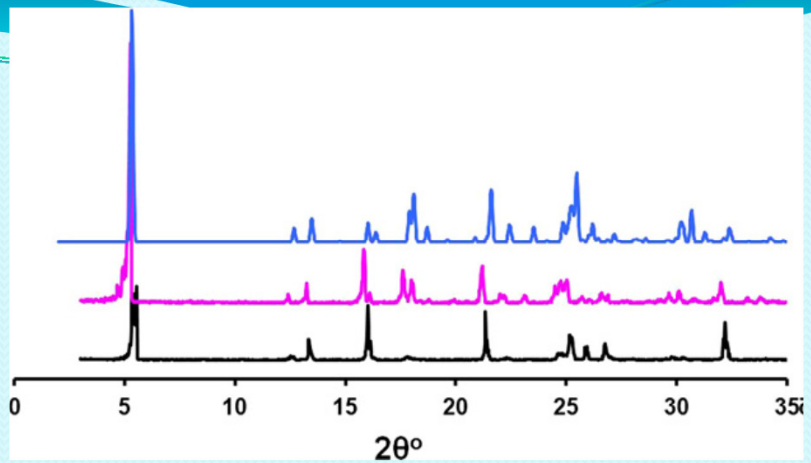

Computed XRPD trace of NTZ calculated at 100 K (a), and experimental traces for the commercial raw powder (NTZ-r) (b) and the crystals obtained from ethyl acetate (NTZ-EA) (c).

ORTEP view of the asymmetric unit of NTZ showing the intramolecular hydrogen bond, atom labeling and non-H atoms drawn as ellipsoids at the 50% probability level (a) and molecular packing in the crystals of NTZ showing the intermolecular C–H O hydrogen bonds, and p-stacking interactions (b).

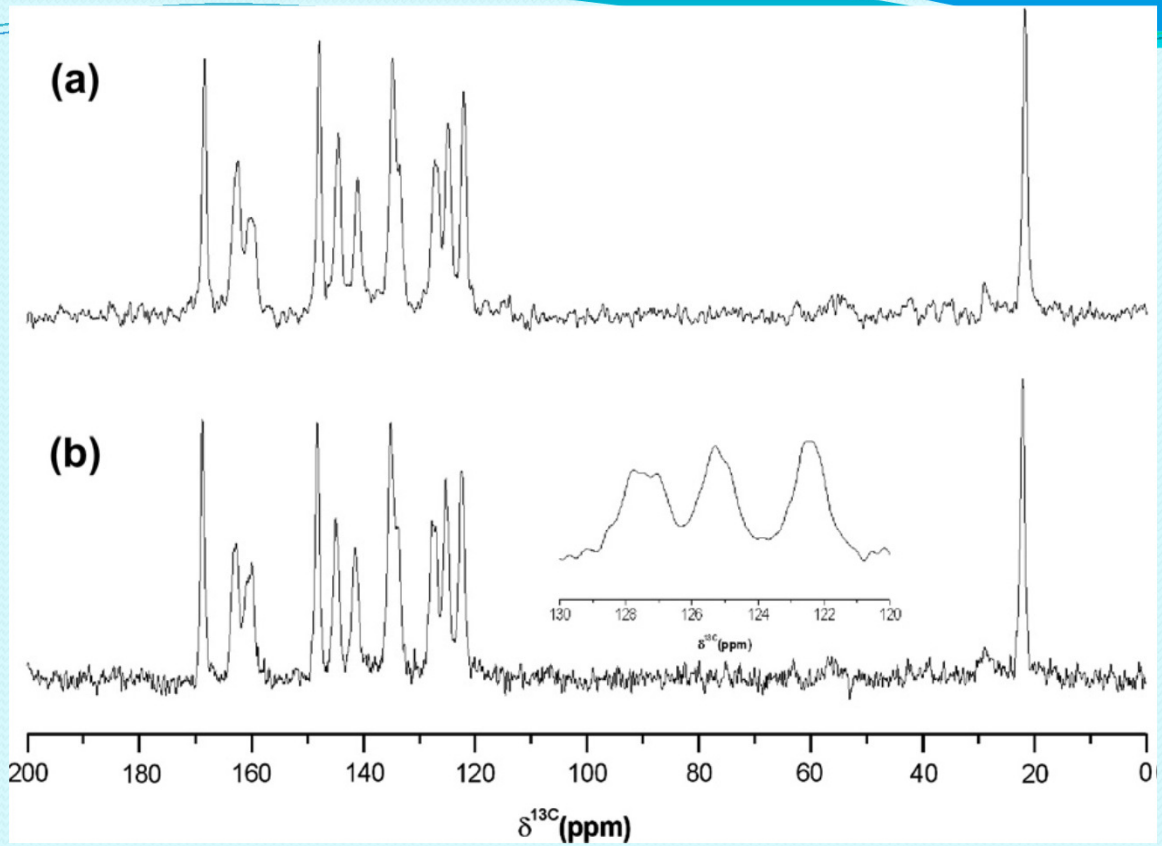

13C CPMAS NMR spectra of NTZ-r (a) and NTZ-EA (b). In the inset the peaks appearing in the 130–120 ppm region are shown.

The 13C SSNMR spectra of NTZ-r and NTZ-EA are very similar, exhibiting well-resolved signals for each C of the molecule. The broadening of the peaks for the 11-carbonyl carbon (163.0 ppm) and C-14 (160.4 ppm)can be attributed to residual dipolar interaction with quadrupolar 14N atoms. Because this interaction depends on the polar angles linking the interatomic distance to the relevant electric field gradient tensor, sometimes the effect is not very noticeable. A splitting of the resonance assigned to C-4 (127.0 and 127.7 ppm) (Fig. 4b and inset), indicates that there are at least two molecules in the asymmetric unit, and this is consistent with the crystallographic data.

APPLICATIONS
POLYMERS

Polyethylene-Polystyrene graft copolymer

Caracterización por 13C-RMN de productos obtenidos por diferentes reacciones de injerto de PS en PE. R. Martini, M. Díaz, G. Monti, S. Barbosa. Simposio Latinoamericano de Polímeros 2008, Lima, Perú, Julio 2008.

MATERIALS

- Polyetilene lineal low density (PE): Mw: 53000 g/mol, PD: 2.9

- Polyestirene (PS): Mw: 270600 g/mol, PD: 1.98

-Two types of reactions:

-Reaction A: in melt

-Reaction B: in solution

Resonance at 126 ppm,characteristic of the *"para"* position show changes, indicating a posible substitution at that position

Characteristic resonances of PE without modifica

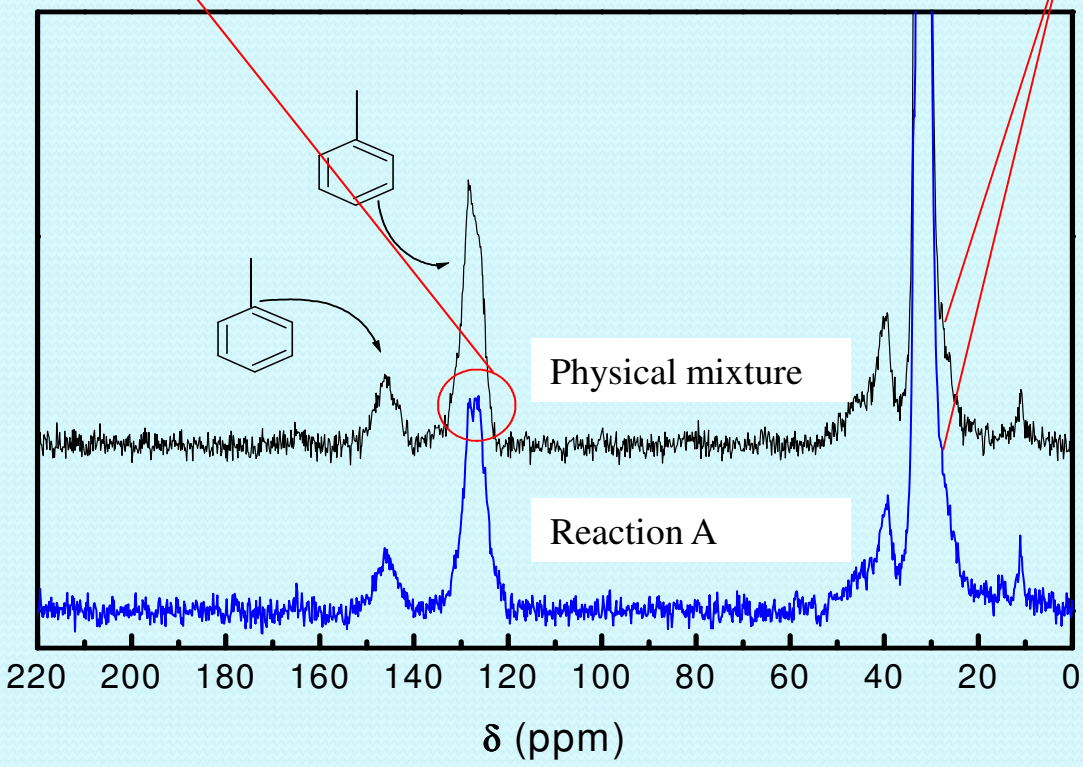

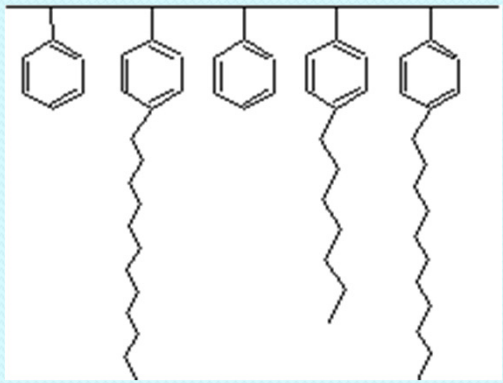

13C-NMR spectrum of products from reaction A compared with a physical mixture

PS formation

Chesaaracteristic resonance of terminal methyl groups of PE are missing in the Reaction B spectrum

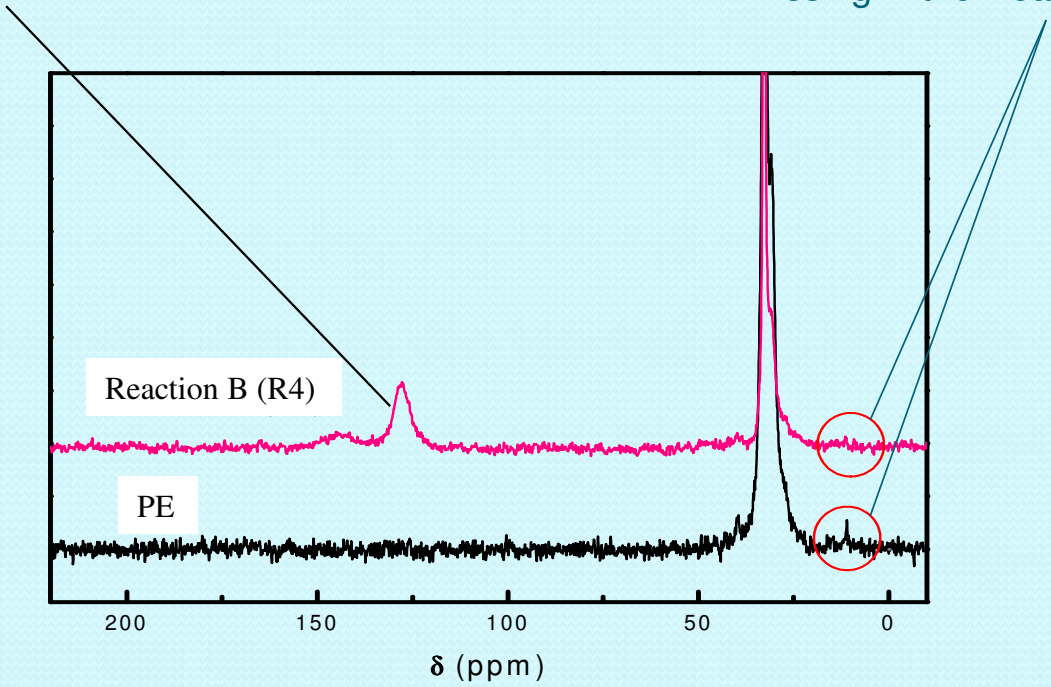

^{13}C-NMR spectrum of the product of the reaction with 4% of $AlCl_3$ compared with PE

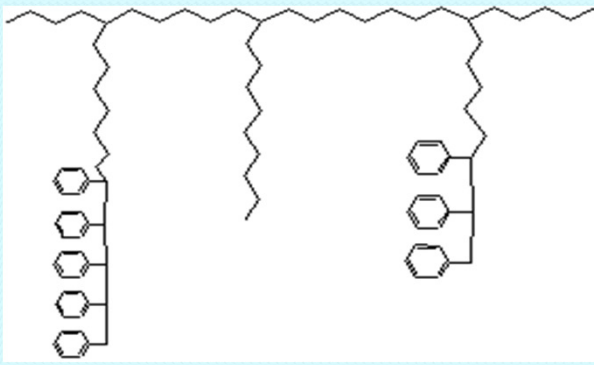

Copper (II) complexes of Polyampholyte and Polyelectrolyte Polymers

New copper(II) complexes of polyampholyte and polyelectrolyte polymers: Solid-State NMR, FTIR, XRPD and thermal analysis. Juan M. Lázaro Martinez, Ana K. Chattah, Gustavo A. Monti, Maria F. Leal Denis, Graciela Y. Buldain, Viviana Campo Dall` Orto. Polymer **49**, 5482–5489 (2008)

Polymer A

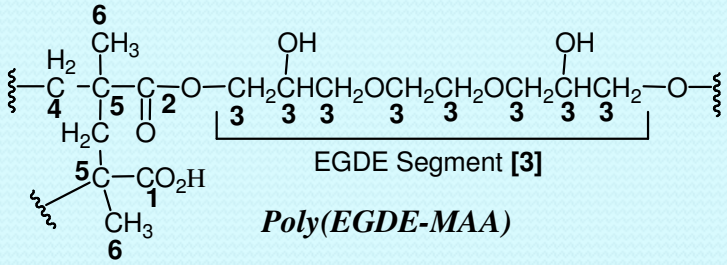

Poly(EGDE-MAA)

Polymer B

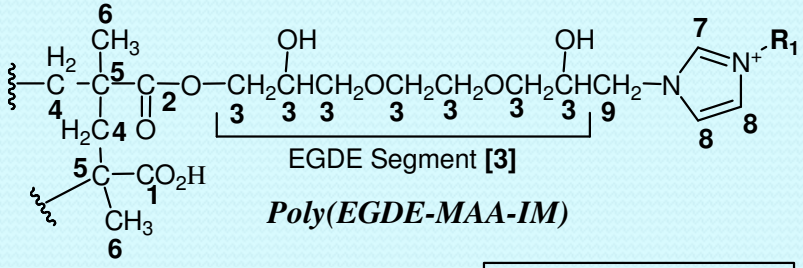

Poly(EGDE-MAA-IM)

R_1 = H or EGDE Segment

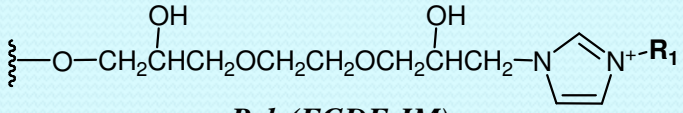

Poly(EGDE-IM)

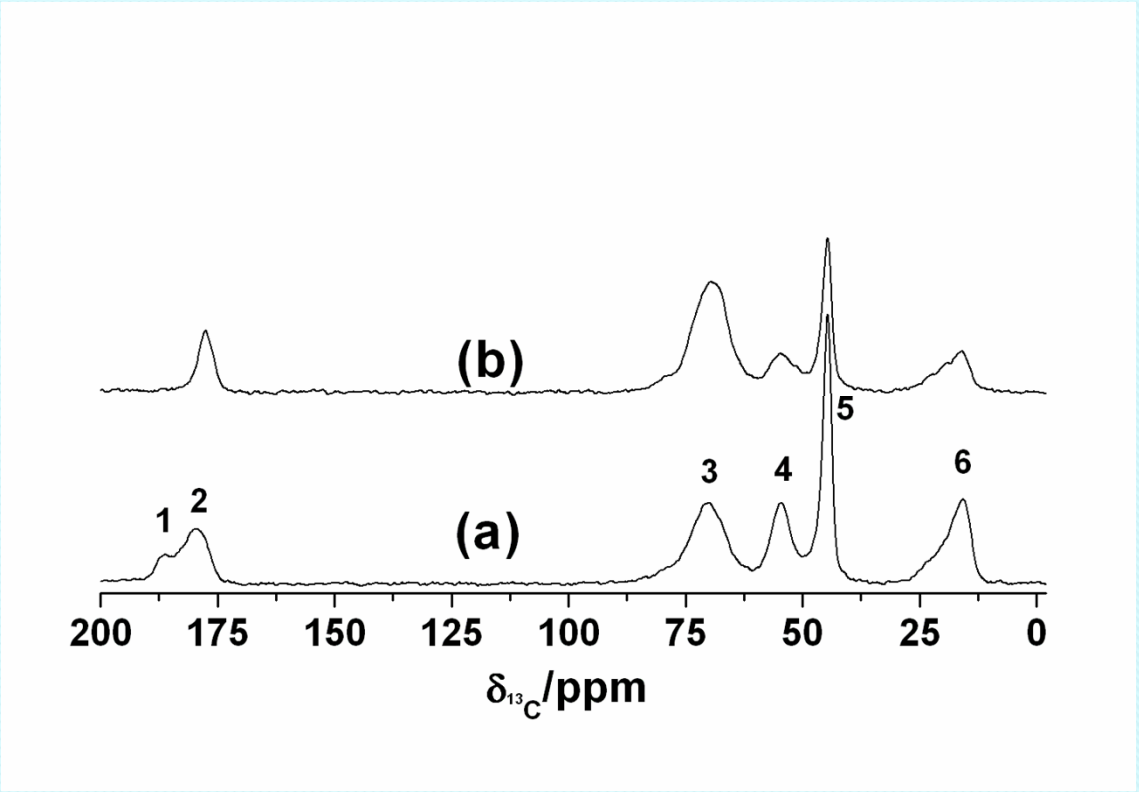

13C CP-MAS spectra of polymer A (a), and its copper complex A1 (b). The numbering corresponds to that in scheme 1. The number of scans for both spectra was 1600.

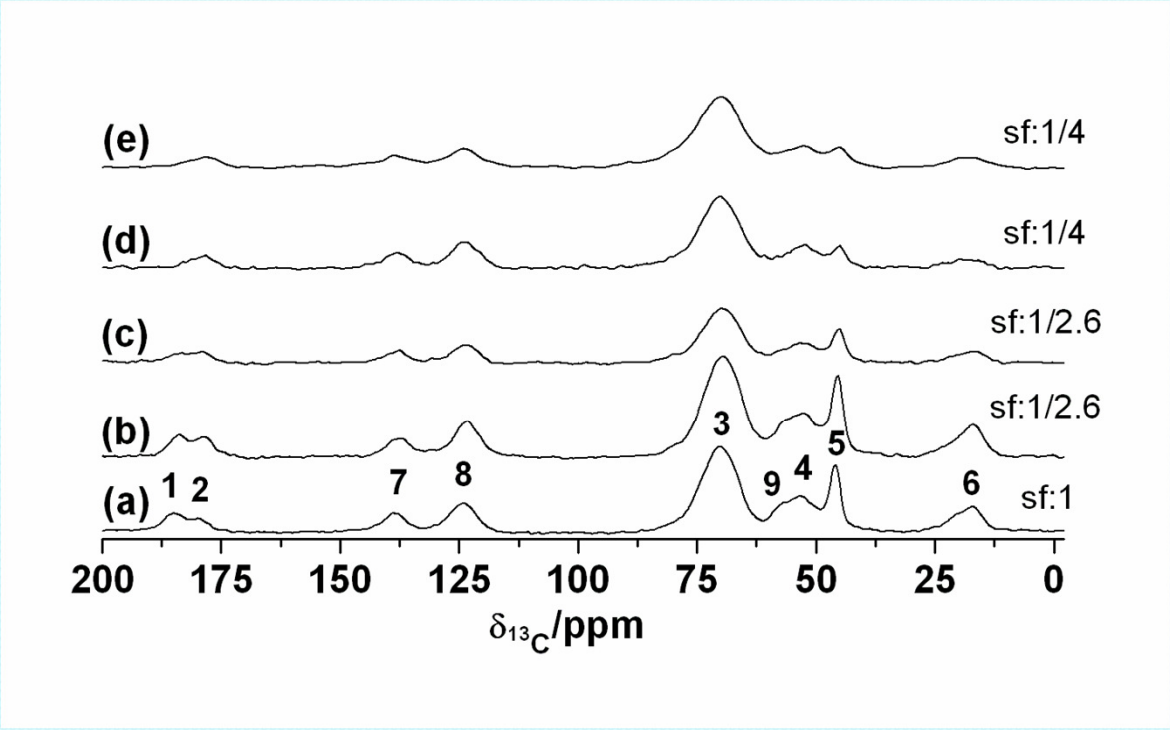

13C CP-MAS spectra of: B (a), and the copper complexes B8 (b), B26 (c), B48 (d) and B63 (e). The labels correspond to those in scheme 1. The number of scans was: 1000 (a), 2600 in (b) and (c), 4000 in (d) and (e). (Sf: Scaling factor).

Discriminating pulse sequences. Spin Diffusion.

Domanin size determination in en PVDF (poly(vinilydene fluoride)) by means of spin diffusion tehcnique [19].

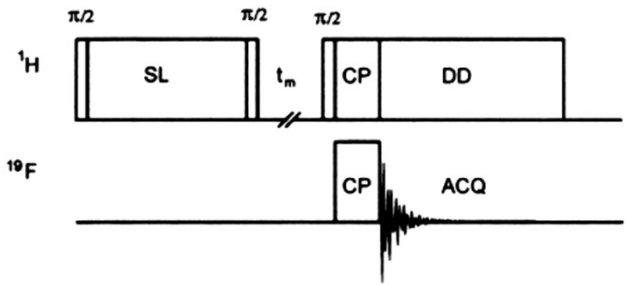

Spin-Lock filter sequence, selection of crystalline components (rigids)

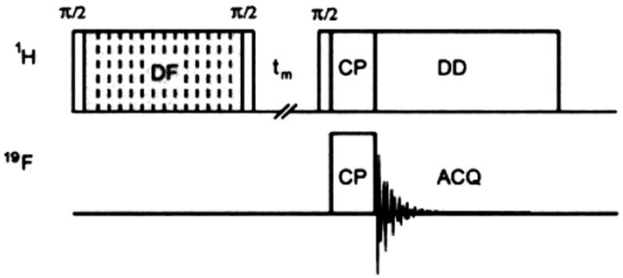

Dipolar filter sequence, selection of amorphous components (mobiles)

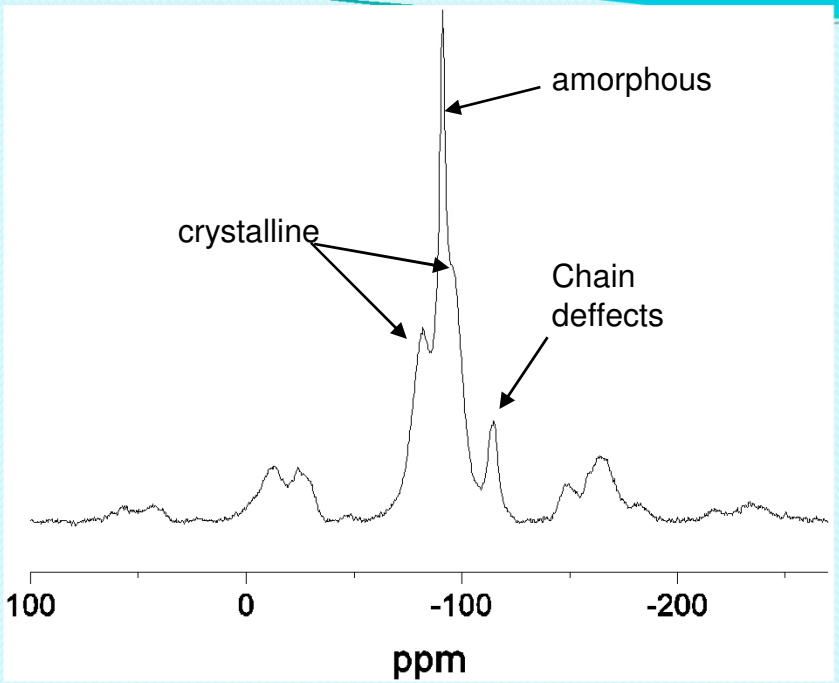

^{19}F NMR spectrum of PVDF non polar α phase 1H→19F CP/MAS 12.5 kHz (P. Holstein et al. 1999). * Rotational bands coming from crystalline regions.

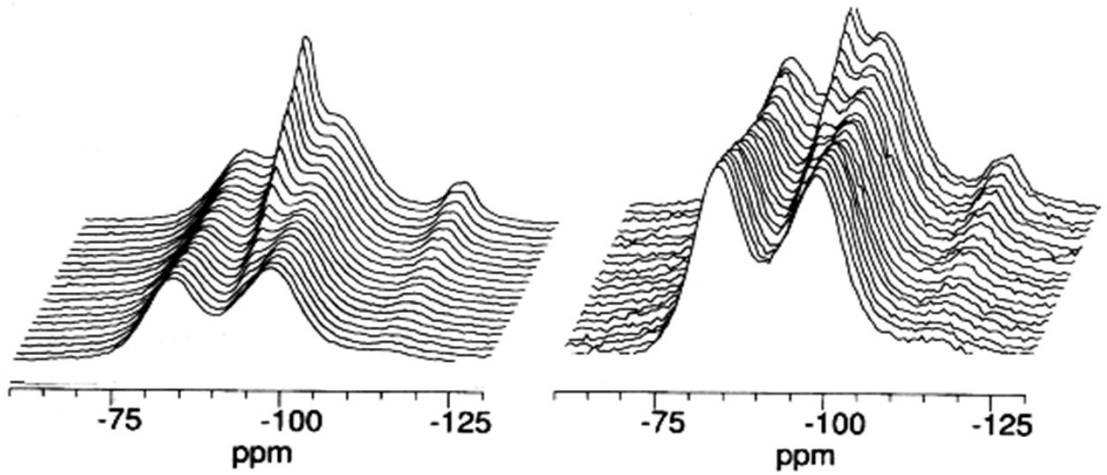

Crystalline phase selection; left contact time 500 μs, right contact time 50 μs

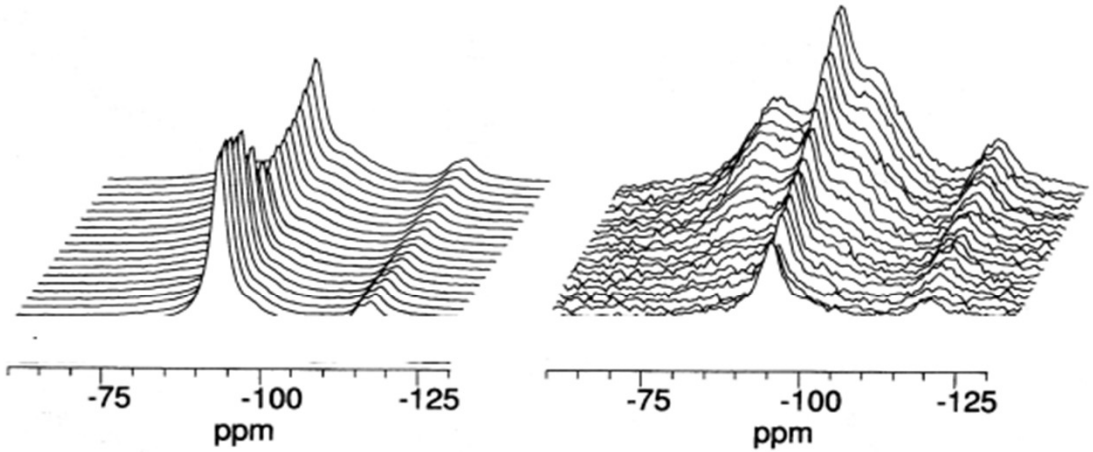

Amorphous phase selection; left contact time 500 μs, right contact time 50 μs

Figure 49: PVDF, ^{19}F spectrum. α phase non polar

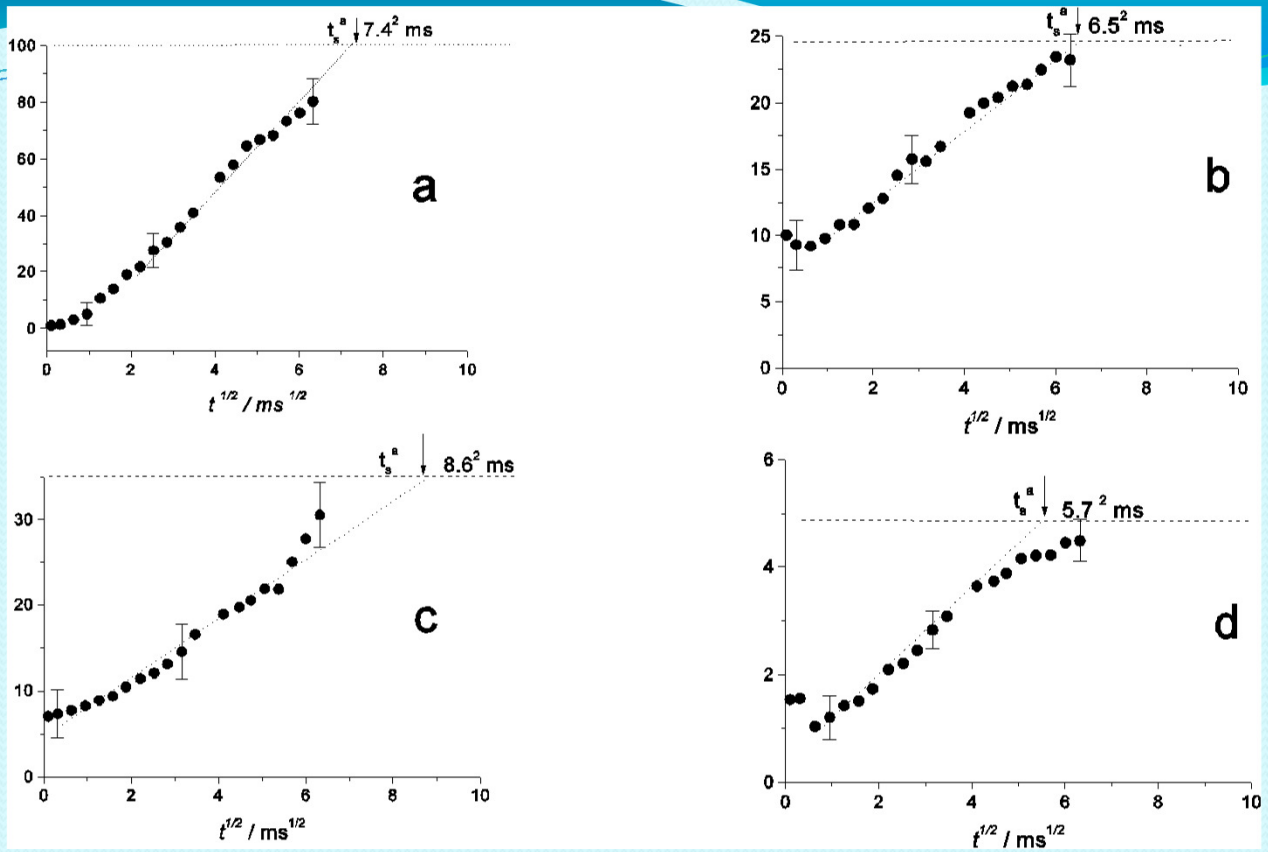

Figure 50: Recovery of ^{19}F magnetization in a spin diffusion experiment with selection of the crystalline phase.

a), b) powder, recovered domain size, amorphous phase, 7.0 ± 0.8 nm

c), d) film, recovered domain size, amorphous phase, 5.7 ± 0.8 nm

(P. Holstein et al. 1999)

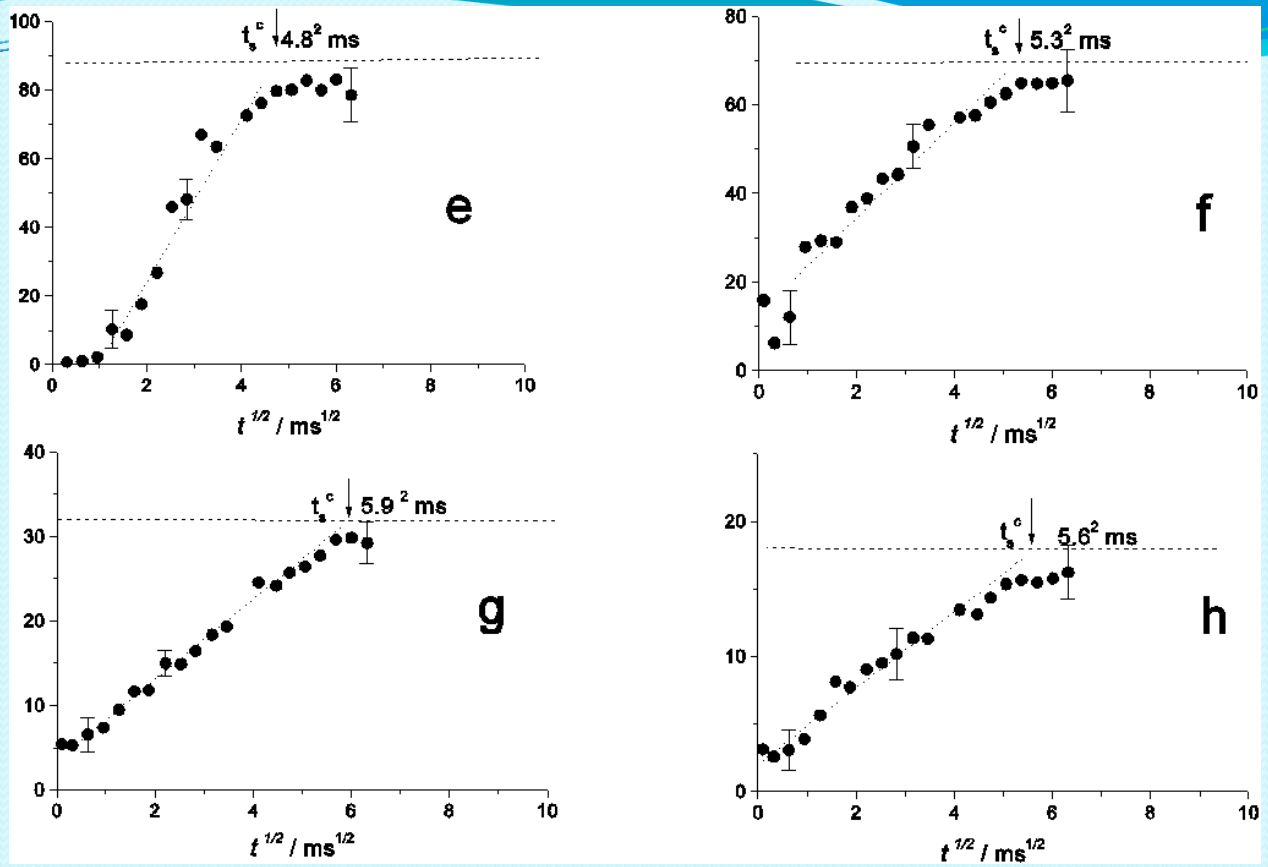

Figure 51: Recovery of ^{19}F magnetization in a spin diffusion experiment with a selection of amorphous phase.

e), f) powder, recovered domain size, crystal phase, 5.2 ± 0.7 nm

g), h) film, recovered domain size, crystal phase, 5.9 ± 0.8 nm

(P. Holstein et al. 1999)